

Annealing-induced structural rearrangement and optical band gap change in Mg-Ni-H thin films

Ž. Rašković-Lovre^{a,b,*}, T. T. Mongstad^a, S. Karazhanov^a, C. C. You^a, S. Lindberg^{a,c}, M. Lelis^d, D. Milcius^d, S. Deledda^a

^a *Institute for Energy Technology, P. O. Box 40, 2027 Kjeller, Norway*

^b *Vinča Institute of Nuclear Sciences, University of Belgrade, P. O. Box 552, 11000 Belgrade, Serbia*

^c *Chalmers University of Technology, SE-412 96, Gothenburg, Sweden*

^d *Lithuanian Energy Institute, LT-44403, Kaunas, Lithuania*

It is well known that optical properties of Mg-Ni-H films can be tuned by hydrogen uptake from Mg-Ni-H and upload into Mg-Ni systems. In this work we show that modulation of optical properties of Mg-Ni-H can take place as a result of thermal processing in air as well. When reactively sputter deposited semiconducting Mg-Ni-H films are annealed at temperatures of 200-300 °C in air, gradual band gap change from 1.6 eV to 2.04 eV occurs followed by change in optical appearance, from brown, to orange and, subsequently, to yellow. We investigate this phenomenon using optical and structural characterization tools, and link the changes to an atomic rearrangement and a structure reordering of the $[\text{NiH}_4]^{4-}$ complex. The films are X-ray amorphous up to 280 °C, where above this temperature an increase in crystallite size and establishing of long-range order lead to a formation of the cubic crystalline phase of Mg_2NiH_4 . Also, the results suggest that even though annealing was conducted in air, no oxidation or other changes in chemical composition of the bulk of the film occurred. Therefore, the band gap of this semiconductor can be tuned permanently by heat treatment, in the range from 1.6 to 2 eV.

Keywords: Metal hydrides, Thin films, Semiconductors, Vapour deposition, Optical properties, X-ray diffraction

1. Introduction

The Mg-Ni-H system has been widely investigated since it features relatively fast sorption kinetics and can store up to 3.6 wt% of hydrogen, which makes it attractive as hydrogen storage material [1,2]. The attention has also been directed towards tailoring of optical properties because of the reversible "switching" properties observed during hydrogen release/ uptake in Mg-Ni-H thin films. With hydrogen uptake, the optical properties change from mirror-like to transparent as a metal-to-semiconductor transition occurs [3].

Studies of the structural properties of Mg_2NiH_4 have showed that the compound can exist in two allotropic forms - a monoclinic or low temperature (LT) one which transforms at ~ 510 K to an anti-fluorite cubic high temperature structure (HT) [4]. Even though LT exists at room temperature, the cubic structure is often detected after synthesis by ball-milling [5], or after induced stress [6] and upon hydrogenation of Mg-Ni thin film systems [7–9].

Different colour manifestations of Mg-Ni-H system have been reported. As *Reilly et al.* showed, the colour of powder samples was red at room temperature [10]. Moreover, Mg_2NiH_4 powder samples can undergo a colour transition due to exposure to air, changing their appearance from orange to brown colour. *Richardson et al.* presented variations in colour for thin films with different Mg to Ni ratio, ranging from bright yellow for Mg-rich compositions to deep red for Ni-rich. The different optical appearance was followed by a change in the estimated values of optical band gap, from 2.4 to 2.8 eV [11]. Furthermore, reported values of band gap for thin films vary from 1.6 to 2.2 eV [7,9,12] and the increase in the band gap width was explained by the presence of a second phase, such as MgH_2 [11,13]. *Blomqvist* and *Noreus* reported that powders of Mg_2NiH_4 can exist in two different LT phase with different colour, the only structural difference being a twinning of the crystal on microscopic level [14].

It is worth mentioning that many of studies of Mg-Ni-H were performed on thin films capped with Pd, where modulation of optical properties takes place as a result of hydrogen uploading/realising through the Pd-capping layer, as well as by variation of Mg to Ni ratio. Therefore, the aim of this study was to investigate the changes in optical properties of thermally treated uncapped Mg-Ni-H films, deposited by reactive sputtering. Distinct from previous reports about reversible color change induced by hydrogen adsorption/desorption or when hydride transform from LT to HT phase (at roughly 240 °C) in the Mg-Ni-H system, we have observed annealing-induced gradient color changes of the films not related to variation of H concentration. Furthermore, we report about amorphous-crystalline or LT-HT transition.

2. Experimental details

2.1. Synthesis of Mg-Ni-H thin films

The thin film samples were prepared by reactive magnetron co-sputtering technique using two targets in different operating modes. The Mg target was set for RF processing with power of 900 W, while the Mg₂Ni target was set in DC mode with a sputtering power of 600 W. Sputtering was performed in a Leybold Optics A550V7 sputtering chamber at room temperature with base pressure $\sim 10^{-6}$ mbar. The deposition was carried out at a constant process pressure of 2×10^{-2} mbar, which was adjusted by Ar (5N) and H₂ (6N) flow. The sample carrier was moved rapidly back and forth through the deposition zone to avoid any gradients in the Mg-Ni composition. The samples were deposited on microscope glass slides (size 26 mm x 76 mm) and were used for investigating their optical, structural and desorption properties. For chemical compositional determination samples were prepared on amorphous polished carbon substrates, while CaF₂ substrates were used for Fourier transform infrared (FTIR) measurements. The

microscope glass and CaF₂ substrates were cleaned with isopropanol. Afterwards, they were dipped into deionized water and kept in an ultrasonic water bath for 15 minutes. Before loading into the pre-chamber, all substrates were dried with a nitrogen gas flow. No capping layer of any sort was applied to the samples. The samples were prepared during the same deposition run.

2.2. Characterisation of Mg-Ni-H thin films

Microstructural characterization of the obtained Mg-Ni-H films was performed by grazing incidence X-ray diffraction (GIXRD) with incident angle of 0.5° using a Bruker D8 Discover setup with Cu-K α radiation ($\lambda=1.5409$ Å). *In situ* X-ray diffraction (XRD) characterization during the annealing process of as-deposited samples was performed with incidence angle of 5° in a Bruker D8 Discover equipped with Bruker MTC-HIGHTEMP chamber. For this type of experiment, the original (parent) sample deposited on microscopic slide was cut in 25 mm x 7 mm pieces. The samples were placed on a Pt:Rh heating foil and the temperature was monitored by an S-type thermocouple laser welded to the backside of the heating foil. The samples were heated from room temperature up to 150 °C with 5 °C min⁻¹ heating rate. After reaching 150 °C samples were left for 20 min to reach thermal equilibrium. Then XRD patterns were recorded using with 5 °C steps. At each temperature step before pattern recording samples were left for 5 min to relax. Single pattern was measured in roughly 25 min. The average crystallite size was estimated from the full width at half-maximum (FWHM) of the diffraction peaks using the Scherrer formula.

The thickness of thin films was determined by KLA-Tencor alpha-step 200 stylus profilometer. The chemical composition of the samples was determined by Rutherford backscattering spectrometry (RBS). The optical transmission and reflection of the films were

measured in the visible spectral range by the Ocean Optics QE65000 optical spectrometer, while *Optical* software [15] was used for a band gap determination. Attenuated total reflection Fourier - infrared spectra were measured with a Bruker Alpha-Platinum IR spectrometer upon a diamond crystal. Spectra were collected in the range $400\text{-}4000\text{ cm}^{-1}$ with resolution of 2 cm^{-1} .

3. Results and discussion

3.1. Annealing of the samples

As-deposited samples were transparent with dark brown colour and did not show a crystalline structure (Fig. 1(a)). The annealing process was conducted in two steps, first at 220 °C, after which the samples were cooled down. The second step was performed at 290 °C. The samples were kept on a heating plate exposed to air for 3 minutes for each annealing step. During this procedure, the colour transition took place twice; once at $T = 220$ °C, as the sample changed colour from dark brown to orange, while remaining amorphous. After cooling down and reheating the sample at $T = 290$ °C, the second colour transition occurred, as the sample became light yellow and crystalline [Inset in Fig. 1(a)].

3.2 Structural characterization

The chemical composition analysis of the 550 nm thick samples deposited on carbon substrates was performed by Rutherford backscattering spectroscopy (RBS). The determined Mg:Ni ratio was 2.5. At all stages, the oxygen signals were close to the background, showing that there was no contamination with O in both as-deposited sample or in the samples annealed in the air. Therefore, we exclude any influence of oxygen on the colour change of the sample. The XRD study showed that the as-deposited brown colour sample, as well as the orange colour sample obtained after the first annealing step, are amorphous or nanocrystalline, with grain sizes below the instrument's detection limit [Fig. 1(a) and 1(b)]. After the second annealing step, when the yellow colour of the sample appeared, XRD revealed polycrystalline structure of Mg_2NiH_4 phase with dominant cubic structural arrangement [Fig. 1(c)].

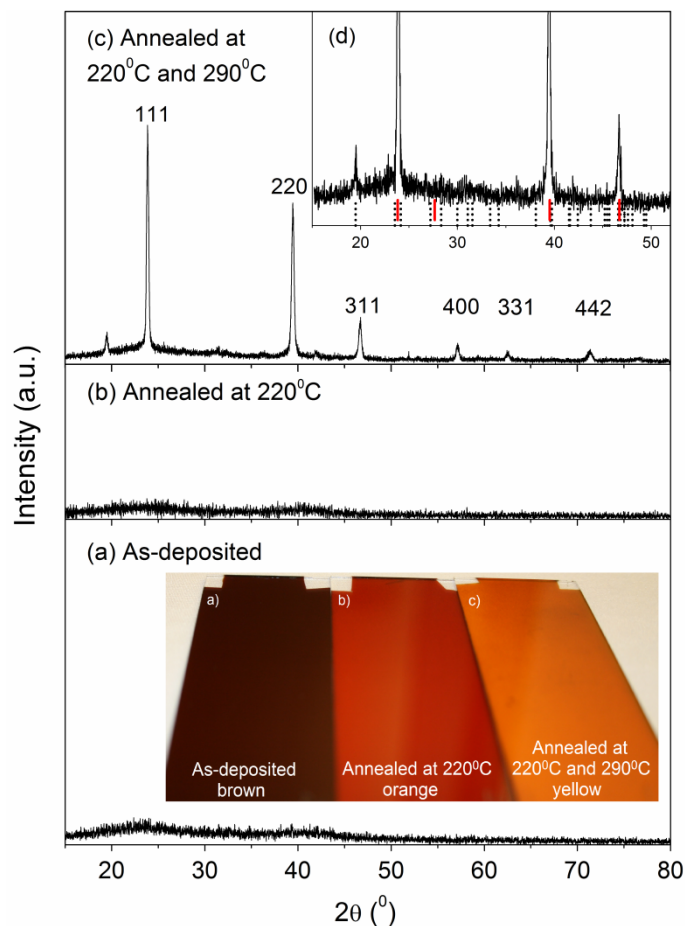


Fig. 1. GIXRD patterns of annealed samples in air: a) as-deposited sample shows amorphous or nanocrystalline structure, b) no visible change in the structure after first annealing step, c) pattern of crystalline yellow sample after second annealing step, which corresponds to HT cubic Mg_2NiH_4 ; d) enlarged pattern of crystalline yellow sample in range of $2\theta = 15-50^\circ$, showing the coexistence of monoclinic and cubic phase. At the bottom standard pattern position of cubic phase are presented with solid lines, whereas the standard positions of monoclinic phase are presented with dash lines. Inset in (a): Photograph of the samples and the colour transitions due to annealing process.

The diffraction peaks corresponded to an *fcc* structure with lattice parameter $a = 6.469 \text{ \AA}$. The two strongest diffraction peaks were detected at $2\theta = 23.82^\circ$ (111) and $2\theta = 39.43^\circ$ (220), which is in agreement with the high temperature (HT) cubic structure of Mg_2NiH_4 [4]. The peak at $2\theta = 19.50^\circ$ observed in Fig. 1(d) could be attributed to the (110) peak of the monoclinic LT phase, suggesting the existence of that phase prior to the first step of annealing. This is in agreement with what reported previously by *Mongstad et al.* [16] who observed signs of a monoclinic structure in a TEM study of reactively sputtered thin films, which were found to be amorphous by XRD. The presence of the (110) peak of LT phase confirms that not all of the crystallites have taken the cubic HT phase as preferred. The structural transformation from nanocrystalline LT to HT and the coexistence of the two structures could be related to the process of annealing. Temperature and time of heating, dwelling time and period of cooling all play an important role in the post-deposited structure and morphology of thin films [17]. Moreover, diffusion of the defects promoting the grain boundaries migration can be stimulated by the transferred heat, also causing the increase of the grain size [18,19]. It can be assumed that growth of grains and structural rearrangement from LT to HT due to the annealing, noticeably affect sample's colour and the colour transition from brown to orange occurs.

The *in situ* XRD data obtained during annealing of the sample in air is shown in Fig. 2. Commonly, upon heating in vacuum, the films desorb hydrogen without crystallization into a phase. Here we found that the first change in the diffraction pattern was visible after the sample reached 280°C . The appearance of the (111) and (220) peaks of the *fcc* HT phase was observed in the range $20^\circ < 2\theta < 40^\circ$ as the temperature increased, Fig. 2(a)-(e).

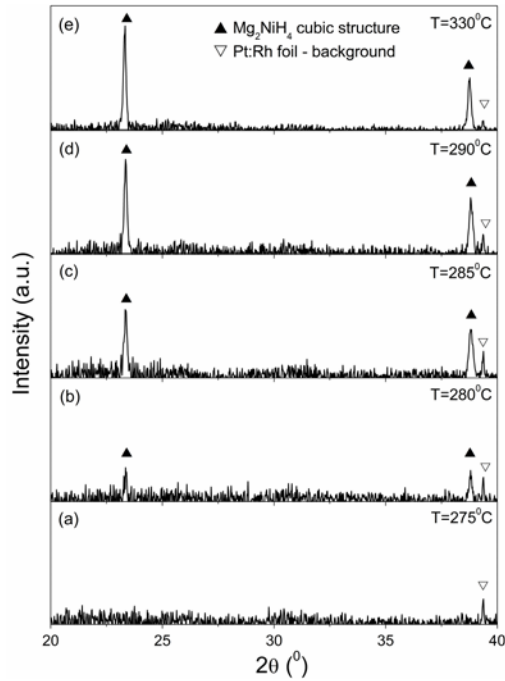


Fig. 2. *In situ* XRD patterns of the sample heated in air: (a-e) (111) and (220) peaks of cubic structure in range of $2\theta = 20-40^\circ$.

According to this finding, the second orange to yellow colour transition happened close to the temperature range as the increase of crystallinity of the sample. The peak at $2\theta = 19.5^\circ$ and the other peaks of the cubic structure at higher values of 2θ are not detected, due to instrumental limit detection. Diffraction peaks corresponding to Mg, MgO and MgH₂ phase were not present, which confirms no formation of large crystalline domains of such phases. The *in situ* XRD measurement was performed until the temperature of the sample has reached 330 °C. No additional peaks that correspond to Mg₂Ni or Mg were observed [Fig. 2(e)]. The overall decrease in the full width at half maximum (FWHM) value of the peaks with the rise of temperature followed by the increase of the crystallites size, from 48.10 to 56.37 nm, was confirmed by using Scherrer equation in the temperature range of 280-330 °C.

3.3 Optical properties

Fig. 3 shows infrared (IR) spectra of Mg-Ni-H system in the range of 400-4000 cm^{-1} for all three colour stages. The spectra of amorphous samples, brown and orange are very similar, while the spectrum of crystalline yellow color sample shows an increase in intensities, as well as a shift of peaks towards higher frequencies.

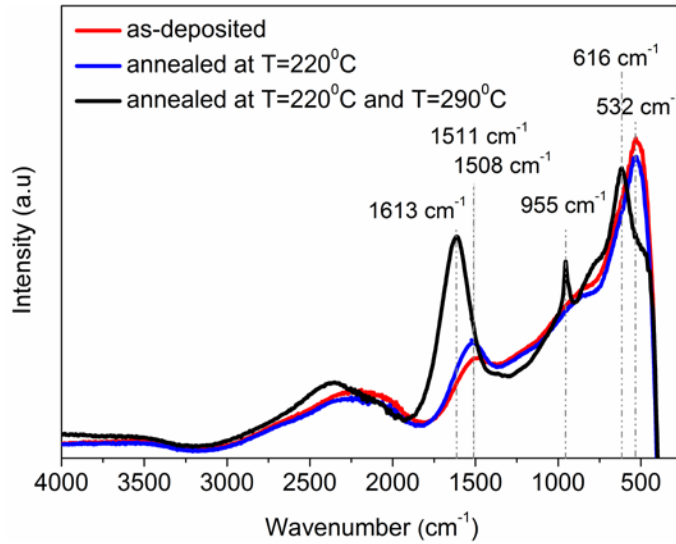


Fig. 3. Infrared spectra of Mg-Ni-H thin film annealed in air measured at room temperature.

Table 1 shows the infrared bands and assignments characteristic to Mg_2NiH_4 bulk material and thin films reported in the literature, along with our results. It can be seen that IR spectra of bulk materials [20] and nanoparticles [9,21] can differ due to influence of the particles size and surface to volume ratio. The broad peak for the brown coloured sample centred at 1508 cm^{-1} is attributed to the ν (Ni-H) stretching mode, whereas the peak at 532 cm^{-1} is attributed to δ (Ni-H) bending mode. The peak of the ν (Ni-H) stretching mode slightly shifts towards higher wavenumber with annealing, to 1511 cm^{-1} , while the other peak remains closely to 532 cm^{-1} . Further, shift and narrowing of the peak follow the second step of the annealing process and the

orange-to-yellow colour transition. The ν (Ni-H) stretching mode is centred at 1613 cm^{-1} and δ (Ni-H) is placed at 616 cm^{-1} in crystalline sample. It can be seen that the Ni-H vibration modes, the peaks' positions and intensities, alter upon annealing. The difference in the positions and intensities of the Ni-H bands demonstrates the change in the local structure in the sample, and most of all that the spectrum is closely related to the Ni-H environment. The latter is governed by the interactive forces between magnesium and nickel atoms, as well as between Mg^{2+} and H^- . The peak of ν (Ni-H) stretching mode becomes narrower with the annealing and can therefore be correlated to the increase in the crystallinity. The blue shift of the peak suggests a change in the rigidity of the Ni-H bond. The Ni-H bands of the yellow sample are similar to the ones reported for the bulk [22], indicating an ordered structure of the complex and the Ni-H bonds as in Mg_2NiH_4 powder. The IR peak at 955 cm^{-1} is attributed to a stretching Mg-H vibration, which corresponds to MgH_2 phase [23]. This narrow peak appeared after the second annealing step at $290\text{ }^\circ\text{C}$. Therefore, the presence of MgH_2 phase in our samples was suggested by the appearance of the peak of Mg-H stretching mode upon grain size increasing.

Table 1. Experimentally measured infrared bands and assignments (cm^{-1}) for Mg-Ni-H. The instrument resolution is $\sim 2\text{ cm}^{-1}$ and the accuracy of the measurement is $\sim 1\text{ cm}^{-1}$.

Assignment	Parker et al. [20]	Lelis et al. [9]	Zhang et al. [21]	Richardson et al. [11]	This study (brown/ orange/ yellow)
ν (Ni-H)	1674^s	1650	1630	1638	$1508/ 1511/ 1612^s$
δ (Ni-H)	791^m	-	-	-	-
δ (Ni-H)	745^m	-	703	-	-
δ (Ni-H)	618^s	-	-	-	$532/ 532/ 616^s$
Libration	528^{sh}	-	-	-	-

^v stretching vibration, ^o bending vibration, ^s strong, ^m medium, ^{sh} shoulder

The reflection and transmission spectra of as-deposited and annealed samples are shown in Figs. 4(a) and 4(b), respectively. After each annealing step the reflection and transmission spectra of Mg-Ni-H films change noticeably. The absorption edge in transmission spectrum of crystalline sample is shifted towards higher energies compared to the spectrum of the as-deposited sample, which indicated to annealing-induced band gap increase. The optical spectra were used to estimate the band gaps of the films. The band gap estimated from fundamental absorption edge of the transmission spectra is 1.6 eV for the as-deposited brown colour film, which is consistent with that of Ref. [7]. A trend of widening of band gap has been observed after each annealing step: 1.83 eV for the orange colour sample and 2.04 eV for the crystalline film. The latter result is in good agreement with the value of 2.08 eV reported in Ref. [24].

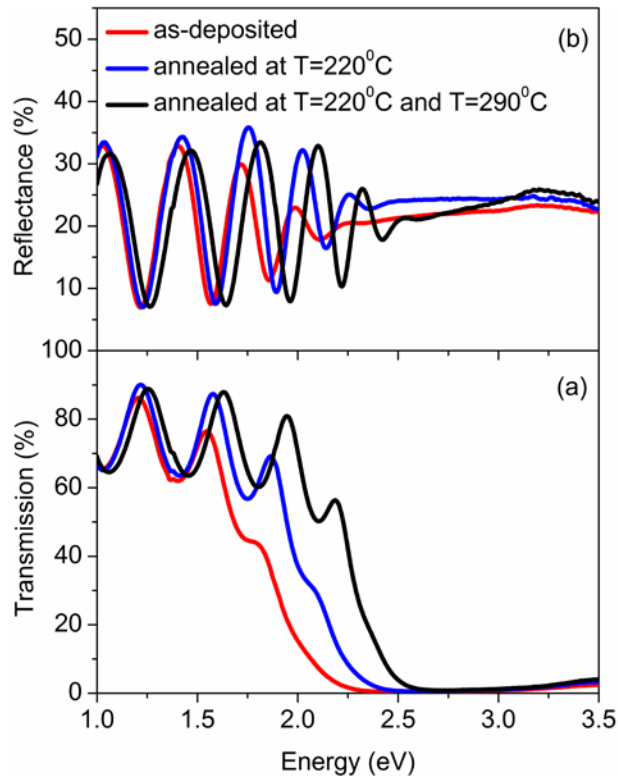


Fig. 4. Transmission (a) and reflectance (b) of three different stages of the 550 nm thick sample of Mg-Ni-H.

It should be noted that the annealing-induced increase of the band gap took place without any chemical change of the composition. The distortion in the Mg sub lattice, firstly from monoclinic to cubic, and later change in the distance of Mg counter ion, has a strong effect on the band gap. The stabilization of $[\text{NiH}_4]^{4-}$ unit and a rigidity of Ni-H bond upon annealing, confirmed by FTIR, also affect the band gap. As shown previously, the H arrangement around the Ni atom has a strong impact on the band gap of Mg_2NiH_4 [25], and the energy gap depends on the separation between energy levels determined by $[\text{NiH}_4]^{4-}$ complex [26]. Indeed, one can expect such result since the valence band maximum of Mg_2NiH_4 is contributed by H *s* electrons whereas the conduction band minimum mainly consists of Ni *d* states (Ref. [25-27]). So, the re-arrangement of the Ni-H bond during thermal processing can be the cause for band gap engineering. On the other hand, the presence and influence of MgH_2 phase cannot be disregarded [11, 13, 28]. As the above analysis shows, the slight discrepancy between the band gaps observed in this work and the ones already published for thin film samples with the similar Mg:Ni ratio, can be explained by the coexistence of other phase.

4. Conclusion

The colour transitions of the Mg-Ni-H system upon annealing in the air were presented and can be related to structural arrangements, the establishment of long-range order and ordering of the structure of the $[\text{NiH}_4]^{4-}$ complex. As-deposited brown colour samples changed colour to orange, after spending 3 minutes on a hot plate at $T=220\text{ }^\circ\text{C}$, while the next transition to yellow appeared after cooling down the samples and heating them again for 3 minutes at $T=290\text{ }^\circ\text{C}$. Our results showed that no chemical change in composition occurred upon annealing of the samples. Distinct from the earlier reported color changes that are related to hydrogen upload into and

uptake from the film, our result takes place at low temperatures below the hydrogen release temperature. So, it is related to internal materials properties and can be explained by heating-induced structural re-arrangement. The thermal treatment resulted in changes of the crystallite size. The formation of MgH_2 during synthesis was confirmed by FTIR measurement. The influence of coexisting MgH_2 can't be excluded and the higher value of the estimated band gap can be attributed to the existence of MgH_2 in the sample. We report about phase transition from amorphous to crystalline phases of Mg-Ni-H. We observed that the band gap of Mg_2NiH_4 semiconductor can be tuned permanently by heat treatment, in the range from 1.6 to 2 eV.

Acknowledgments

This research was financially supported by Ministry of Education and Science of Republic of Serbia, under grant III 45012, by the Research Council of Norway through the Yggdrasil mobility program 2012 - 219352/F11, the ISP project 181884 and FRINATEK, and from internal project funding at Institute for Energy Technology. The Research Council of Norway is acknowledged for the support to the Norwegian Micro- and Nano-Fabrication Facility, NorFab (197411/V30). The authors would like to thank to O. Zavorotynska for FTIR measurement and V. Venkatachalapathy for the technical support. The authors wish to thank Professor E. S. Marstein and Dr. S. E. Foss for fruitful discussions and support.

* Corresponding author.

Tel: +381 652139503. E-mail address: zeljka.raskovic@vinca.rs (Ž. Rašković-Lovre).

References

- [1] S. Orimo, H. Fujii, Effects of nanometer-scale structure on hydriding properties of Mg-Ni alloys: a review, *Intermetallics*. 6 (1998) 185–192.
- [2] M. Polanski, T.K. Nielsen, I. Kuncce, M. Norek, T. Płociński, L.R. Jaroszewicz, et al., Mg₂NiH₄ synthesis and decomposition reactions, *Int. J. Hydrogen Energy*. 38 (2013) 4003–4010.
- [3] R. Gremaud, J.L.M. Van Mechelen, H. Schreuders, M. Slaman, B. Dam, R. Griessen, Structural and optical properties of Mg_yNi_{1-y}H_x gradient thin films in relation to the as-deposited metallic state, *Int. J. Hydrogen Energy*. 34 (2009) 8951–8957.
- [4] Z. Gavra, M.H. Mintz, G. Kimmel, Z. Hadari, Allotropic Transitions of Mg₂NiH₄, *Inorg. Chem*. 18 (1979) 3595–3597.
- [5] R. Martínez-Coronado, M. Retuerto, J.A. Alonso, Simplified mechano-synthesis procedure of Mg₂NiH₄, *Int. J. Hydrogen Energy*. 37 (2012) 4188–4193.
- [6] E. Ronnebro, J.O. Jensen, D. Noreus, N.J. Bjerrum, Structural studies of disordered Mg₂NiH₄ formed by mechanical grinding, *J. Alloys Compd.* 293-295 (1999) 146–149.
- [7] J. Isidorsson, I.A.M.E. Giebels, M. Di Vece, R. Griessen, Electrochromism of Mg-Ni hydride Switchable Mirrors, *Proc. SPIE*. 4458 (2001) 128–137.
- [8] E. Wirth, D. Milcius, L.L. Pranevicius, D. Noreus, T. Sato, C. Templier, Influence of ion irradiation effects on the hydriding behavior of nanocrystalline Mg–Ni films, *Vacuum*. 81 (2007) 1224–1228.
- [9] M. Lelis, D. Milcius, E. Wirth, U. Hålenius, L. Eriksson, K. Jansson, et al., A mechanically switchable metal-insulator transition in Mg₂NiH₄ discovers a strain sensitive, nanoscale modulated resistivity connected to a stacking fault, *J. Alloys Compd.* 496 (2010) 81–86.
- [10] J.J. Reilly, R.H.J. Wiswall, The reaction of hydrogen with alloys of magnesium and nickel and the formation of Mg₂NiH₄, *Inorg. Chem*. 7 (1968) 2254–2256.
- [11] T.J. Richardson, J.L. Slack, R.D. Armitage, R. Kostecki, B. Farangis, M.D. Rubin, Switchable mirrors based on nickel-magnesium films, *Appl. Phys. Lett.* 78 (2001) 3047–3049.

- [12] J.H. Selj, T. Mongstad, B.C. Hauback, S.Z. Karazhanov, The dielectric functions and optical band gaps of thin films of amorphous and cubic crystalline Mg_2NiH_4 , *Thin Solid Films*. 520 (2012) 6786–6792.
- [13] P. Van der Sluis, M. Ouwerkerk, P.A. Duine, Optical switches based on magnesium lanthanide alloy hydrides, *Appl. Phys. Lett.* 70 (1997) 3356–3358.
- [14] H. Blomqvist, D. Noréus, Mechanically reversible conductor–insulator transition in Mg_2NiH_4 , *J. Appl. Phys.* 91 (2002) 5141–5148.
- [15] E. Centurioni, Generalized matrix method for calculation of internal light energy flux in mixed coherent and incoherent multilayers., *Appl. Opt.* 44 (2005) 7532–7539.
doi:10.1364/AO.44.007532.
- [16] T. Mongstad, C.C. You, A. Thogersen, J.P. Maehlen, C. Platzter-Björkman, B.C. Hauback, et al., $\text{Mg}_{1-y}\text{Ni}_y(\text{H}_x)$ thin films deposited by magnetron co-sputtering, *J. Alloys Compd.* 527 (2012) 76–83.
- [17] H.S. Chin, L.S. Chao, The effect of thermal annealing processes on structural and photoluminescence of zinc oxide thin film, *J. Nanomater.* 2013 (2013) 1–9.
- [18] C. V. Thompson, R. Carel, Texture development in polycrystalline thin films, *Mater. Sci. Eng. B.* 32 (1995) 211–219.
- [19] P.B. Barna, M. Adamik, Growth mechanisms of polycrystalline thin films, *Sci. Technol. Thin Film.* (1995) 1–28.
- [20] S.F. Parker, K.P.J. Williams, T. Smith, M. Bortz, B. Bertheville, K. Yvon, Vibrational spectroscopy of tetrahedral ternary metal hydrides: Mg_2NiH_4 , Rb_3ZnH_5 and their deuterides, *Phys. Chem. Chem. Phys.* 4 (2002) 1732–1737.
- [21] H. Zhang, X.L. Wang, Y.Q. Qiao, X.H. Xia, J.P. Tu, Microstructure, hydrogenation and optical behavior of Mg-Ni multilayer films deposited by magnetron sputtering, *Appl. Surf. Sci.* 257 (2011) 5759–5765.
- [22] N. Huang, H. Yamauchi, J. Wu, Q.D. Wang, Determination of Hydrogen Atom Configurations in Mg_2NiH_4 by Entropy Considerations and Infrared Spectra, *Z. Phys. Chem.* 163 (1989) 225–230.
- [23] J.R. Santisteban, G.J. Cuello, J. Dawidowski, A. Fainstein, H.A. Peretti, A. Ivanov, et al., Vibrational spectrum of magnesium hydride, *Phys. Rev. B.* 62 (2000) 37–40.

- [24] W. Lohstroh, R.J. Westerwaal, J.L.M. van Mechelen, H. Schreuders, B. Dam, R. Griessen, The dielectric function of Mg_yNiH_x thin films ($2 \leq y \leq 10$), *J. Alloys Compd.* 430 (2007) 13–18.
- [25] W.R. Myers, L.-W. Wang, T.J. Richardson, M.D. Rubin, Calculation of thermodynamic, electronic, and optical properties of monoclinic Mg_2NiH_4 , *J. Appl. Phys.* 91 (2002) 4879–4885.
- [26] G.N. Garcia, J.P. Abriata, J.O. Sofo, Calculation of the electronic and structural properties of cubic Mg_2NiH_4 , *Phys. Rev. B.* 59 (1999) 11746–11754.
- [27] S. Z. Karazhanov, A. Ulyashin. Similarity of electronic structure and optical properties of Mg_2NiH_4 and Si! *Euro Phys. Lett.* **82**(4), (2008), 48004.
- [28] I.A.M.E. Giebels, J. Isidorsson, R. Griessen, Highly absorbing black Mg and rare-earth-Mg switchable mirrors, *Phys. Rev. B.* 69 (2004) 205111–1.